P10.119 RADAR FORWARD OPERATOR FOR DATA ASSIMILATION AND MODEL VERIFICATION FOR THE COSMO-MODEL

Ulrich Blahak[2], Yuefei Zeng[1], Dorit Epperlein[1]

[1] Institute for Meteorology und Climate Research, Karlsruhe Institute of Technology (KIT)

[2] German Weather Service (Deutscher Wetterdienst, DWD)

1 INTRODUCTION

A new radar forward operator for simulating terrestrial weather radar measurements from NWP model output is currently developed. It is suitable for a broad range of applications like, e.g., radar data assimilation in the framework of Ensemble Kalman Filter Systems, or verification of cloud microphysical parameterizations. This operator calculates the radar observables reflectivity and radial wind (later also polarisation parameters) from the prognostic model output. The rationale is to have a comprehensive radar simulator, which comprises all relevant physical aspects of radar cloud measurements in a quite accurate way, but at the same time to provide the possibility for simplifications in a modular fashion. This enables the user to configure and tailor the operator for special applications, that is, to find the "best" balance between physical accuracy and computational effort.

This operator is currently implemented as a module in the non-hydrostatic fully compressible state-of-the-art NWP model of the Consortium for Small Scale Modeling (COSMO), called "COSMO-model" (formerly "Lokal Modell" LM; Doms and Schättler, 2002; Baldauf et al., 2011). COSMO is a cooperation of 7 European National Meteorological Services, and Germany is one of the partners. More information can be found online at **http://www.cosmo-model.org**.

The new weather radar network of the DWD comprises 17 C-Band dual polarisation Doppler radar systems evenly distributed throughout Germany for complete coverage. They provide unique information about cloud structure and precipitation in three dimensions and high spatial and temporal resolution. Up to now these data are not used in the operational COSMO-model of DWD, except within the framework of the latent heat nudging and for a simple nudging method of the radial wind. Future applications are however planned to make better use of radar data within an upcoming new LETKF data assimilation system (Hunt et al., 2007), which will be based on a convection-allowing high resoluton ensemble forecasting system (grid spacing 2.8 km over Central Europe, 40 members, 8 runs a day out to +21 h). Here, the use of weather radar data is a promising means for improvements of the model initial state for short-term precipitation forecasts.

However, the observations (reflectivity, radial velocity, polarisation parameters) are not directly comparable to the prognostic variables of the model (hydrometeor mass contents and sometimes number densities). But the above-mentioned LETKF-assimilation system has the property to be able to work with data directly in measurement space instead of model space with the help of forward operators. So this will be an important future application of our radar forward operator. On the other hand, a more common application is to compare the output of numerical simulations with radar observations in the context of cloud microphysics verification.

Given this planned range of applications, the radar forward operator has to be applicable on supercomputer architectures in an operational environment, and efficiency is a major design criterion, which requires for good parallelization and vectorization properties of the code. This is different to other radar forward operators on the market. Because the COSMO-model (like most of the state-of-the-art NWP models) is written in Fortran 95, this programming language is also applied for our radar operator.

2 Design of the forward operator

The basic purpose of a radar forward operator is to simulate the measurement process of radar observables like radial wind v_r, equivalent reflectivity factor Z_e or polarisation parameters within the "virtual reality" of an NWP model. For the sake of simplicity, we will only refer to v_r and Z_e in the remainder of this paper, but generalisation to polarisation parameters should mostly be straight-forward. For now, we restrict ourselves to terrestrial radars which do volume scans in horizontal mode, i.e., consecutive azimutal sweeps at different fixed elevation angles.

The main ingredients of radar simulation are depicted schematically in Figure 1. Here, the green mesh symbolizes a typical grid configuration of an NWP model, overlayed over the typical measuring volume of a weather radar along a bended ray path. Backscattering and extinction effects are symbolized by arrows, and the beam weighting function is shown on the right.

Mathematically, the radar measurement operators for

* *Corresponding author address:* Ulrich Blahak, Deutscher Wetterdienst, Frankfurter Straße 135, 63067 Offenbach Germany; e-mail: ulrich.blahak@dwd.de

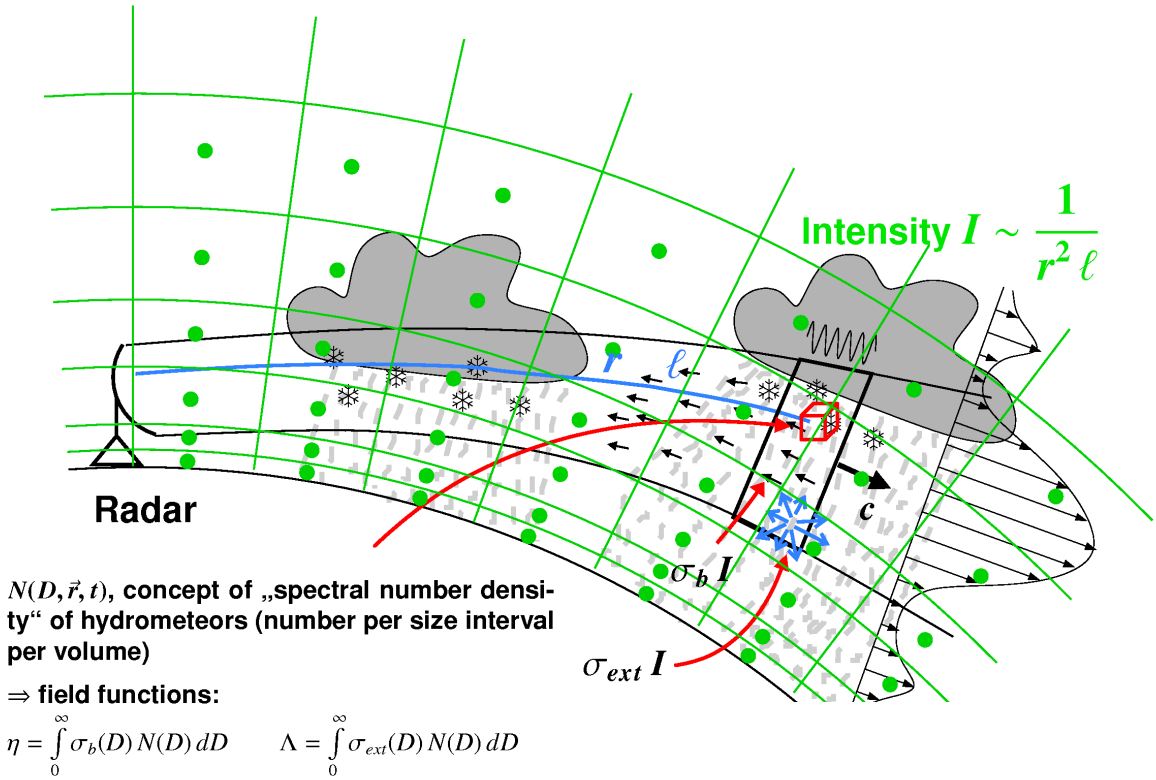

Fig. 1: Conceptual sketch of the relevant physical processes and properties of a radar measurement along a single ray path, overlayed with a typical discrete grid representation of variables in an NWP model (green).

reflectivity and radial wind can be written as spatial weighted averages in the in quite general form as given in Figure 3, Equation (5) – (4), where the superscript$^{(R)}$ denote ”radar measured” and the equations are for a single radar pulse volume which is centerd around a distance r_0 from the radar. The explanation of the various symbols can be found in the figure caption. Note that we take into account only a simplified "box-car" range weighting function. It also has to be mentioned that one arrives at the present formulation for $Z_e^{(R)}$ only if one assumes the two-way beam weighting function f^4 to be Gaussian, an assumption which enters the picture, because the radar processor assumes this when converting the measured power values to output values for Z_e^R.

Note also that we have presented the operator equations relative to the ”beam system”, i.e., distance along ray path r, and horizontal and vertical angles ϕ and θ relative to the ray in the beam center, see Figure 2 (a ”beam” can be thought of consisting of an infinite number of rays bundled within the pulse volume). In this quasi-spherical system, the beam center is situated in the equator plane.

However, measured radar data from volume scans (the ones we want to simulate ultimately) are usually given in the ”radar system”, radial distance r, azimut α and elevation ε, where these angles are measured relative to the antenna azimut and elevation angles α_0 and ε_o. This is different from the beam system in that the equatorial plane is the tangential plane to the earth surface, and both systems are tilted with respect to each other. Figure 2 shows a simplified sketch of the different beam- and radar coordinates.

To take this into account, the operator equations are transformed from the beam system to the radar system using approximations given by Blahak (2008a). Also, we have so far neglected that output values in radar data sets are usually averages over many consecutive pulses and, at the same time, rotating antenna to achieve statistical signal stability. As shown by Blahak (2008a), this leads to a somewhat broader effective beam weighting function f_e^4.

Both effecs ultimately result in a ”name change” $\phi \rightarrow \alpha$, $\theta \rightarrow \varepsilon$ in the integrals and replacment of f^4 by f_e^4. The resulting operator for $\langle Z_e^{(R)} \rangle$ is given in Figure 4, Equation (7). The same f_e^4 is also applied to v_r. Note that the azimutal reference coordinate for the averaged data values is now α_*, the center of the averaging interval $\Delta\alpha$, over which the many pulses at different α_0-values habe been averaged.

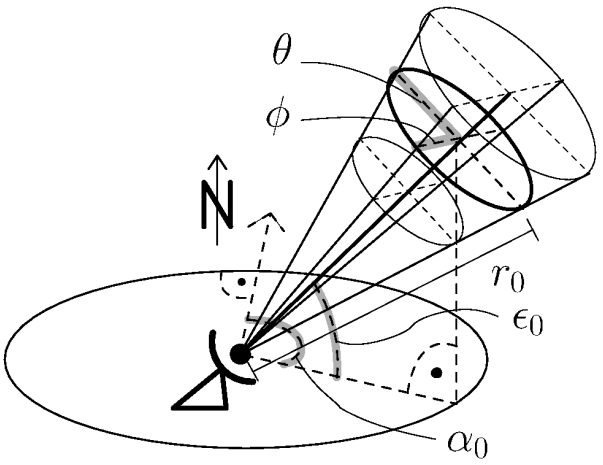

Fig. 2: Conceptual sketch of the different coordinate systems: "beam system" consisting of r, ϕ, and θ; "radar system" consisting of r, α, and ε. For simplicity, only r_0, α_0 and ε_0 of the pulse volume center are shown in this figure, but each point in space can be referenced by either (r, ϕ, θ) or (r, α, ε).

Generally, the task of radar simulation can be devided into two sub-tasks:

1) Compute the field functions v_r and Z_e from the modeled hydrometeor fields. In the COSMO-model, if applying one of the "standard" one-moment cloud schemes, these are the mass densities L_x, $x \in$ {cloud drops, rain drops, cloud ice, snow, graupel}. In case of applying the implemented Seifert-Beheng two-moment cloud microphysical scheme, there is also a hail class and number densities M_x for all species (Seifert and Beheng, 2006; Seifert et al., 2006; Blahak, 2008b; Noppel et al., 2010). To compute v_r and Z_e, the particle size distributions (PSDs) of the species are derived from the model variables in a model-consistent way, i.e., using the same assumptions for the PSDs (generalized gamma distribution) and on the mass-size- and fallspeed-size-relations (power laws) as in the model, so that σ_b and σ_{ext} can be integrated over the size distributions and summed up over all species to get Z_e and the attenuation coefficient Λ.

2) "Radar sampling" of these field functions taking into account the most relevant characteristics of a radar measurement: beam bending by atmospheric refraction, attenuation (integral over Λ along the travel path to a specific location within the pulse volume), beam function weighted volume averaging, and shadowing by orographic obstacles.

For task 1), we decided to compute v_r and Z_e on the native grid of the NWP model and interpolate these quantities to the polar radar grid to subsequently perform task 2). This leads to the flow chart depicted in Figure 5.

The computation of σ_b and σ_{ext} is based on full Mie-scattering and temperature dependent refractive index of the particles and is described in detail in Blahak (2007). It is possible to switch to simpler and computationally more efficient formulas employing the Rayleigh approximation together with simple approximations for the refractive index. Special care is given to partially melted particles: the user may choose from different Effective Medium Approximations (EMA) for the effective refractive index of ice-water-air mixtures, and from different melting models for cloud ice, snow, graupel, and hail, which are either based on one- or two-layered spheres.

No polarization parameters are computed yet, but we intend to implement code for one-layered spheroidal particles in the future, with help of code from Pfeifer et al. (2008). However, this will drastically increase the computational effort, so that it is necessary to simplify the computations, e.g., by the use of lookup tables, which cover the relevant range of the basic parameters (T, L_x, M_x, local elevation) and depend on assumptions about canting angle distributions and axis ratios of the spheroids as function of size.

For task 2), beam bending is computed based on Snell's law for a continuous spherically stratified medium, and the refractive index is computed as a function of temperature T, pressure p and vapor pressure e. Optionally, to save numerical effort, the well-known "4/3-earth" approximation (based on standard atmospheric conditions, constant in time) is implemented as an alternative.

For pulse-volume-averaging in azimutal and elevational direction, efficient Gauss-Legendre quadrature is employed, with a selectable number of integration points. The integrals are evaluated within the 90-% total energy range of the two-way beam function, i.e., $\pm 1.29\,\theta_3/2$ centered around the beam axis. Values from the model grid are interpolated linearily to the positions on the radar grid, which are determined by the computed ray paths, antenna azimuts and elevations and necessary auxiliary interpolation points needed for the Gauss-Legendre quadrature.

As mentioned earlier, a realistic range weighting (e.g., "matched filter") is not taken into account so far, but radar measurables are rather computed only at the mid distances r_0. Although technically not difficult, it has not been implemented yet because, for our typical applications, the horizontal model grid spacing is larger than the radar range bin, so that range weighting would have nearly no effect. However, this is not necessarily the case for averaging in the other directions, especially in the vertical (elevational), where the model grid spacing can be as small as 100 – 300 m or even less.

Optionally, the elevational and/ or azimutal averaging can be switched off to save computing time, in which

Basic field functions for the radar operator:

$$\text{Reflectivity } \eta: \qquad \eta(r,\phi,\theta) \;=\; \int_0^\infty \sigma_b(D)\,N(D,r,\phi,\theta)\,dD \tag{1}$$

$$\text{Attenuation coefficient } \Lambda: \qquad \Lambda(r,\phi,\theta) \;=\; \int_0^\infty \sigma_{ext}(D)\,N(D,r,\phi,\theta)\,dD \tag{2}$$

$$\text{Effective reflectivity factor:} \qquad Z_e(r,\phi,\theta) \;=\; \eta(r,\phi,\theta)\,\frac{\lambda^4}{\pi^5\,|K_{w,0}|^2} \tag{3}$$

$$\text{Reflectivity weighted average fall speed of hydrometeors:} \qquad \bar{v}_T \;=\; \frac{\int_0^\infty \sigma_b(D)\,N(D)\,v_T(D)\,dD}{\eta} \tag{4}$$

Radar operator for effective reflectivity factor Z_e in "beam system", single beam:

$$Z_e^{(R)}(r_0) \;=\; \frac{\int_{r_0-c\tau/4}^{r_0+c\tau/4}\int_{-\pi}^{\pi}\int_{-\pi/2}^{\pi/2} Z_e(r,\phi,\theta)\;\overbrace{\exp\left(-2\int_0^r \Lambda(r',\phi,\theta)\,dr'\right)}^{\ell_n^{-2}(r,\phi,\theta)}\;\frac{f^4(\phi,\theta)}{r^2}\cos\theta\,d\theta\,d\phi\,dr}{\int_{r_0-c\tau/4}^{r_0+c\tau/4}\int_{-\pi}^{\pi}\int_{-\pi/2}^{\pi/2} \frac{f^4(\phi,\theta)}{r^2}\cos\theta\,d\theta\,d\phi\,dr} \tag{5}$$

with ℓ_n^{-2} beeing the path integrated attenuation by precip from the radar to location (r,ϕ,θ).

Radar operator for radial velocity in "beam system", single beam:

$$\begin{aligned} v_r^{(R)}(r_0) \;&=\; \frac{\int_{r_0-c\tau/4}^{r_0+c\tau/4}\int_{-\pi}^{\pi}\int_{-\pi/2}^{\pi/2} \ell_n^{-2}\left(\int_0^\infty \sigma_b(D)N(D,r,\phi,\theta)\;[(\vec{v}-v_T(D)\vec{e}_3)\cdot\vec{e}_r]\,dD\right)\frac{f^4(\phi,\theta)}{r^2}\cos\theta\,d\theta\,d\phi\,dr}{\int_{r_0-c\tau/4}^{r_0+c\tau/4}\int_{-\pi}^{\pi}\int_{-\pi/2}^{\pi/2} \frac{\eta(r,\phi,\theta)}{\ell_n^2}\frac{f^4(\phi,\theta)}{r^2}\cos\theta\,d\theta\,d\phi\,dr} \\ &=\; \frac{\int_{r_0-c\tau/4}^{r_0+c\tau/4}\int_{-\pi}^{\pi}\int_{-\pi/2}^{\pi/2} (\vec{v}\cdot\vec{e}_r)\,\frac{\eta}{\ell_n^2}\frac{f^4}{r^2}\cos\theta\,d\theta\,d\phi\,dr}{\int_{r_0-c\tau/4}^{r_0+c\tau/4}\int_{-\pi}^{\pi}\int_{-\pi/2}^{\pi/2} \frac{\eta}{\ell_n^2}\frac{f^4}{r^2}\cos\theta\,d\theta\,d\phi\,dr} \;-\; \frac{\int_{r_0-c\tau/4}^{r_0+c\tau/4}\int_{-\pi}^{\pi}\int_{-\pi/2}^{\pi/2} (\vec{e}_3\cdot\vec{e}_r)\,\bar{v}_T\,\frac{\eta}{\ell_n^2}\frac{f^4}{r^2}\cos\theta\,d\theta\,d\phi\,dr}{\int_{r_0-c\tau/4}^{r_0+c\tau/4}\int_{-\pi}^{\pi}\int_{-\pi/2}^{\pi/2} \frac{\eta}{\ell_n^2}\frac{f^4}{r^2}\cos\theta\,d\theta\,d\phi\,dr} \end{aligned} \tag{6}$$

Fig. 3: Equations for the radar operator in quite general form. Spatial coordinates are given in the "beam system", i.e., distance along ray path r, horizontal and vertical angles ϕ and θ relative to the radar beam center ray. r_0 is the distance to the pulse volume center, f^4 is the two-way beam weighting function, $N(D)$ is the particle size distribution (PSD) as function of diameter D, σ_b the backscattering coefficient, σ_{ext} the extinction coefficient, $\vec{v}$ the wind vector, v_T the terminal fall speed of hydrometeors, $\vec{e}_3$ the unit vector upwards perpendicular to the earth surface, and $\vec{e}_r$ the unit vector in radial ray path direction.

Radar operator for Z_e in "radar system" taking into account azimutal averaging:

$$\langle Z_e^{(R)} \rangle (r_0, \alpha_*, \varepsilon_0) = \frac{\int_{r_0-c\tau/4}^{r_0+c\tau/4} \int_{\alpha_*-\pi}^{\alpha_*+\pi} \int_{\varepsilon_0-\pi/2}^{\varepsilon_0+\pi/2} Z_e(r,\alpha,\varepsilon) \exp\left(-2\int_0^r \Lambda(r',\alpha,\varepsilon)\,dr'\right) \frac{f_e^4(\alpha,\varepsilon)}{r^2} \cos\varepsilon\, d\varepsilon\, d\alpha\, dr}{\int_{r_0-c\tau/4}^{r_0+c\tau/4} \int_{\alpha_*-\pi}^{\alpha_*+\pi} \int_{\varepsilon_0-\pi/2}^{\varepsilon_0+\pi/2} \frac{f_e^4(\alpha,\varepsilon)}{r^2} \cos\varepsilon\, d\varepsilon\, d\alpha\, dr} \quad (7)$$

with f_e^4 = effective beam weighting function of an azimutally scanning radar:

$$f_e^4(\alpha,\varepsilon) = \exp\left\{-8\ln 2\left(\left(\frac{(\alpha-\alpha_*)\cos\varepsilon}{\alpha_{3,eff,0}+(\cos\varepsilon_0-1)\Delta\alpha\,(1-\exp(-1.5\,\Delta\alpha/\theta_3))}\right)^2 + \left(\frac{\varepsilon-\varepsilon_0}{\theta_3}\right)^2\right)\right\} \quad (8)$$

Fig. 4: Equations for the Z_e-operator transformed to the "radar system", along with the effective beam weighting function f_e^4 of an azimutally scanning weather radar after Blahak (2008a). An inherent assumption herein is that the single-beam antenna pattern has been approximated by the usual Gaussian function. $\langle Z_e^{(R)} \rangle$ represents an average value over several consecutive pulses α_* is the center of the averaging interval (usually "the" azimut in a radar data set), $\Delta\alpha$ is the averaging intervall of the consecutive pulses, θ_3 is the 3-dB-oneway beam width, and $\alpha_{3,eff,0}$ is the effective 3-dB-oneway beam width at 0 elevation, which only depends on the radar specific ratio $\Delta\alpha/\theta_3$ and can be deduced by interpolation from Table 1 of Blahak (2008a).

case the radar measurables are taken as linearily interpolated values on the centerlines of the (bended) beams.

The following additional processes are neglected so far:

- attenuation by atmospheric gases → is already corrected for in most radar signal processors),
- aliasing of v_r into the Nyquist-range (could be implemented easily),
- radar miscalibration → not exactly known for most radar systems,
- attenuation by wetted radome,
- and probably others.

3 Computational issues

Applicability of the code on parallel and vector machines is a major design criterion, as well as computational efficiency. This is a very important topic in the context of our development work, but it is mainly a technical matter. Nonetheless, a few aspects shall be mentioned in this paper.

The task of simulating an arbitrary number of radars has to be parallelized in order to perform well on supercomputers, and the parallelization has to be done in a way that each computing processor gets about equal work to do, to achieve a good load balancing and avoid idle times of single processors.

The strategy of the COSMO-model (and most NWP models) is to divide the simulation domain horizontally in a number of cubes with equal base area, so that each processor computes the time integration of the model equations only for such a sub-domain and there is comparable work load per processor. Communication between "neighbouring" processors is necessary in each time step, because the finite-difference calculation of horizontal gradients at the domain boundaries requires the exchange of data values across domain borders. However, for current supercomputer architectures, this communication can be very time consuming, so it is wise to avoid commmunication as much as possible.

Within this domain decomposition, the radar bins (polar coordinates) including the auxiliary grid points for the numerical quadrature of a specific radar might be distributed asynchroneously over different neighbouring processor domains: for regions close to the radar, the bins are much denser distributed as compared to far away from the radar, and the number of bins per processor region depends on the radar position. This is a source of some load imbalance. However, the first

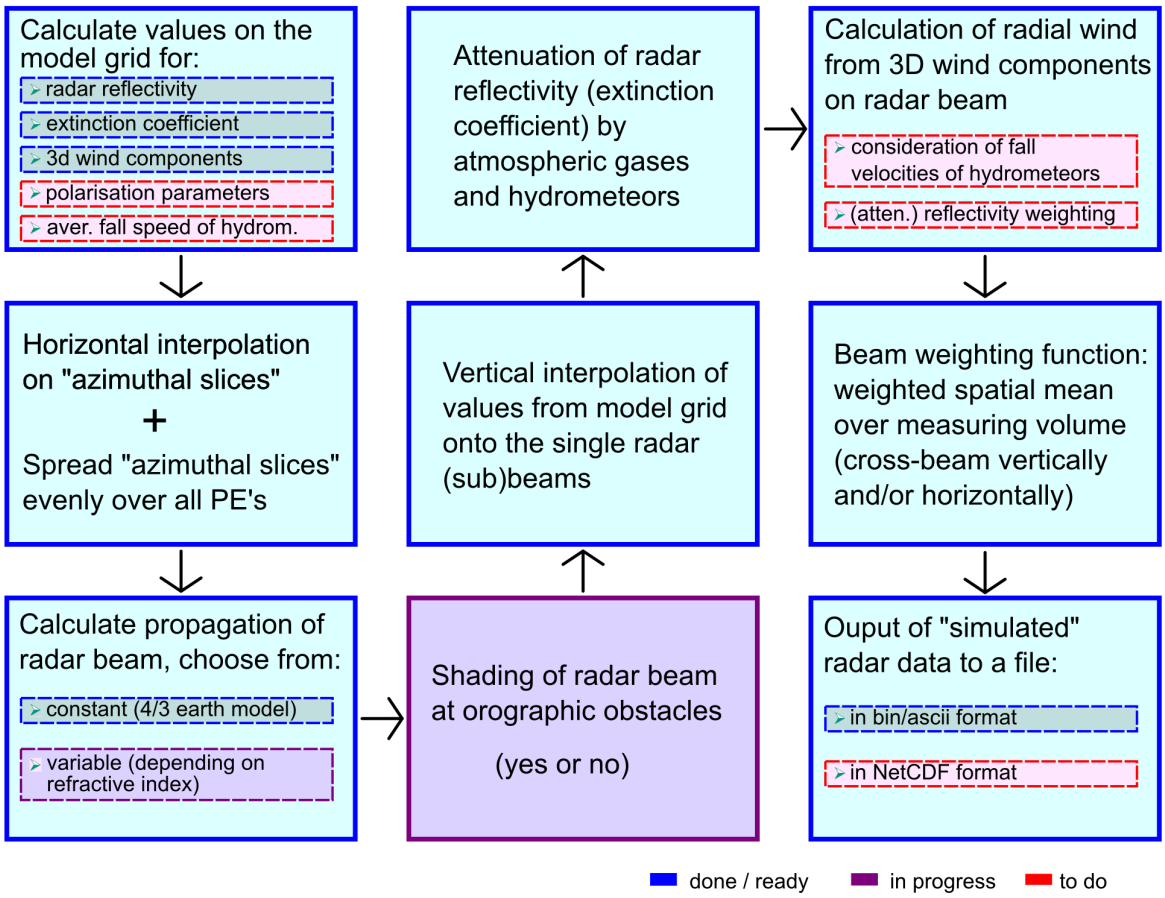

Fig. 5: Conceptual flow chart of the radar forward operator. The different colors denote the different stages of development: blue = done, purple = in progress, red = to do.

step of radar simulation is to compute some field functions on the radar grid and then to interpolate them to the locations of the radar bins, and load imbalances cannot be totally avoided. The premise here is to minimize the computations involved in this step.

The last step be the output of the data of single radar stations to separate files, which means that these data have to be collected to a single processor for writing to a file. What is done inbetween these steps depends on the type of beam propagation computation. If the time-constant 4/3-earth model is applied, the horizontal positions and heights of the radar bins can be computed only based on the bin coordinates, and interpolated data can be collected directly to one output processor per radar station. There, re-sorting into regular 3D arrays, summing up the attenuation along single ray paths and computing the averaging integrals can be performed before output. If there are considerably less radar stations than processors, this can be very imbalanced, but it restricts the costly communication to a minimum.

If, however, the beam propagation (height of radar bin as function of distance) is computed every time step base on actual refractive index values, a second communication step is necessary, because the method involves the iterative computation of radar heights along each ray path from the radar site outwards. To aviod processors waiting for the results of others and to ease the organization of communication, an auxiliary grid consisting of vertical "azimutal slices" centered around the radar stations is defined, and all slices from all radars are distributed evenly over the processors. After communicating the necessary interpolated data to these slices, beam propagation respectively radar bin heights can be computed independently on each processor, and the radar quantities can be interpolated in the vertical to these heights. Then, essentially the same collection of whole radar station data sets on single output processors and attenuation and integration computations follow as for the time-constant beam propagation. The additional communication step is costly, but it leads to a well balanced computation of beam propagation.

A main improvement could be, if it would be possible to organize the output of the data to radar station files in a somewhat different way, so that each processor (not only 1 processor per station) could be involved here. However, no good solution has been found until now.

4 First results and conclusions

First simulations with a development version of the new radar forward operator and the COSMO-model have been performed on the NEC SX9 vector-parallel supercomputer of DWD. One exemplary result is presented in the following to conclude this paper.

In an idealized framework, a convective system is triggered by a warm bubble at $t = 0$ within environmental conditions similar to those described by Weisman and Klemp (1982). The horizontal model grid spacing has been chosen to 1 km with a time step of 6 s. One radar station is simulated with volume scans every 5 minutes (20 elevation, 360 azimuts, 130 range bins of 1 km each). After about two hours, a large squalllline-type system has evolved from the cold forward outflow (coldpool) of an inital pair of rotating supercells. In a layer up to about 2 km AGL, large raindrops dominate the hydrometeor "mix", whereas partially melted graupel and supercooled raindrops co-exist in the adjacent layer up to about 6 km height. Above, dry graupel- and smaller cloud ice particles are present.

Figure 6 compares modeled Z_e-values from this time on PPI-surfaces at an elevation of 4.5°, obtained with different configurations of the reflectivity calculation and at the two wavelengths 5.5 cm and 3 cm.

It can be seen that using a most simple analytic Rayleigh approximation (no attenuation) for all species (computationally very cheap) leads to essentially the same results at the two different wavelengths, as it should be. Considering full Mie-scattering without attenuation leads to stronger reflectivities. In this case, the effect is mainly due to a much better representation of the partially melted graupel, using a suitable EMA (Maxwell-Garnett) for the refractive index of the melting particles for the Mie scattering cross sections. For the analytic Rayleigh formulation above, a much simpler formula (Oguchi, 1983) has been used, which is known to be problematic for ice-water-air mixtures due to the largely different refractive index values of water and ice/air.

When taking further the attenuation by hydrometeors into account, Z_e-values are considerably reduced, and the effect is stronger at the shorter wavelengths, as it was to be expected. The strong attenuation in this case is again caused by the partially melted graupel particles, whose extinction cross sections are much larger that those of raindrops of the same mass.

All in all, the first development version of the forward operator seems to produce promising results. Simulations with more than one radar have also been performed and revealed no fundamental problems. When using the Rayleigh approximation, computing times for the operator are usually smaller than those for the "rest" of the model.

However, the program is not complete yet (e.g., polarisation parameters missing), and more work has to be invested in making the Mie-scattering computations more efficient, which, at the moment, increase the computation time of the radar operator by approximately one order of magnitude.

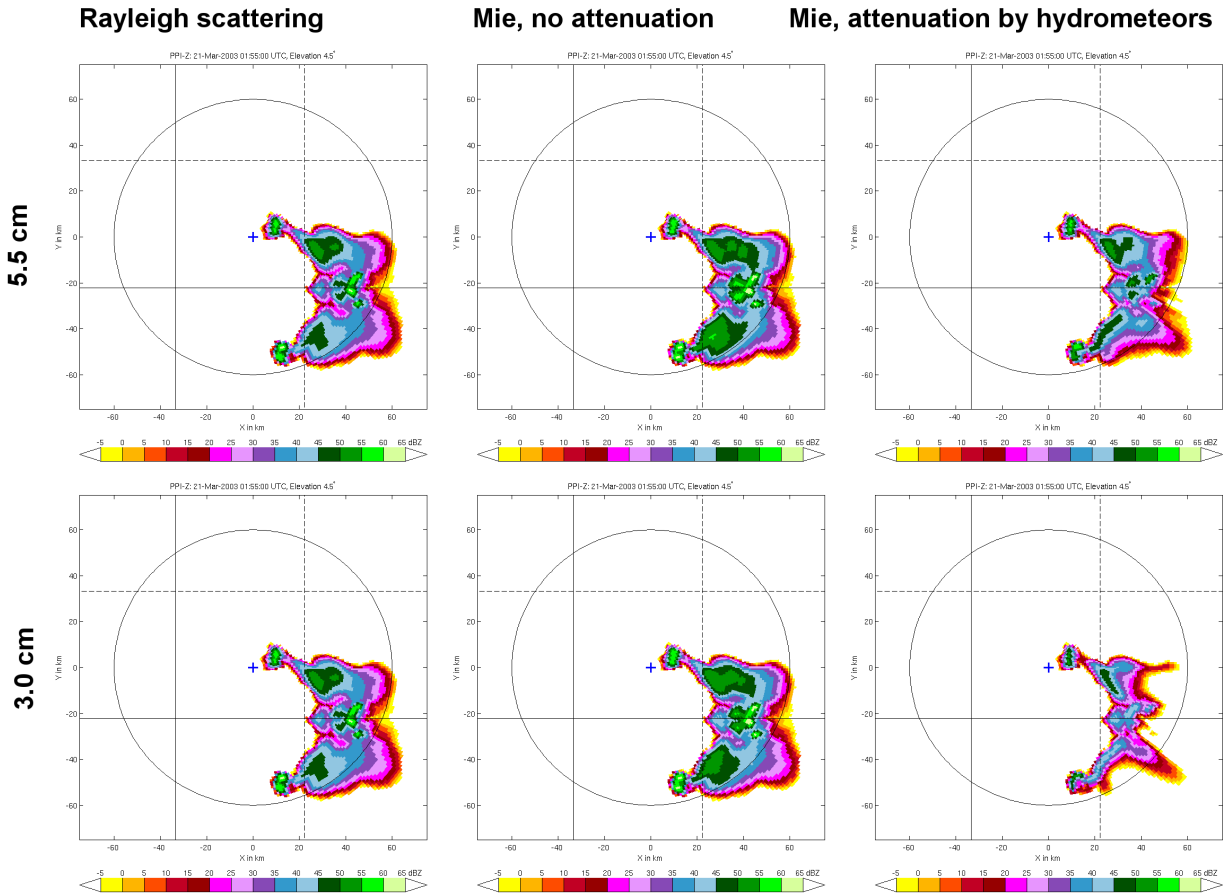

Fig. 6: Idealized study (see text): modeled Z_e-values from $t = 2$ h for $\varepsilon_0 = 4.5°$ (PPI), obtained with different configurations of the reflectivity calculation (columns) and at the two wavelengths 5.5 cm and 3 cm (rows).

REFERENCES

Baldauf, M., A. Seifert, J. Förstner, D. Majewski, M. Raschendorfer and T. Reinhardt, 2011: Operational convective-scale numerical weather prediction with the COSMO model: description and sensitivities, *Mon. Wea. Rev.*, DOI: 10.1175/MWR-D-10-05013.1.

Blahak, U., 2007: RADAR_MIE_LM and RADAR_MIELIB — calculation of radar reflectivity from model output, *Internal report, Inst. f. Meteor. and Climate research, University/ Research Center Karlsruhe*, available on request, 167 p.

Blahak, U., 2008a: An approximation to the effective beam weighting function for scanning meteorological radars with axisymmetric antenna pattern, *J. Atmos. Ocean. Tech.*, **25**, 1182–1196.

Blahak, U., Towards a better representation of high density ice particles in a state-of-the-art two-moment bulk microphysical scheme, Extended Abstract, International Conference on Clouds and Precipitation, Cancun, 7.7. – 11.7.2008, 2008b, online: http://cabernet.atmosfcu.unam.mx/ICCP-2008/abstracts/Program_on_line/Poster_07/Blahak_extended_1.pdf.

Doms, G. and U. Schättler, 2002: *A Description of the Nonhydrostatic Regional Model LM. Part I: Dynamics and Numerics*, Consortium for Smallscale Modeling (COSMO), available online: http://www.cosmo-model.org/content/model/documentation/core/cosmoDyncsNumcs.pdf, 134 pp.

Hunt, B. R., E. J. Kostelich and I. Szunyogh, 2007: Efficient data assimilation for spatiotemporal chaos: A local ensemble transform kalman filter, *Physica D: Nonlinear Phenomena*, **230**(1-2), 112 – 126.

Noppel, H., U. Blahak, A. Seifert and K. D. Beheng, 2010: Simulations of a hailstorm and the impact of CCN using an advanced two-moment cloud microphysical scheme, *Atmos. Res.*, **96**, 286–301.

Oguchi, T., 1983: Electromagnetic wave propagation and scattering in rain and other hydrometeors, *Proc. IEEE*, **71**(9), 1029–1078.

Pfeifer, M., G. C. Craig, M. Hagen and C. Keil, 2008: A polarimetric radar forward operator for model evaluation, *J. Appl. Meteor. Clim.*, **47**, 3202–3220.

Seifert, A. and K. D. Beheng, 2006: A two-moment cloud microphysics parameterization for mixed-phase clouds. Part I: Model description, *Meteorol. Atmos. Phys.*, **92**, 45–66.

Seifert, A., A. Khain, A. Pokrovsky and K. D. Beheng, 2006: A comparison of spectral bin and two-moment bulk mixed-phase cloud microphysics, *Atmos. Res.*, **80**, 46–66.

Weisman, M. L. and J. B. Klemp, 1982: The dependence of numerically simulated convective storms on vertical wind shear and buoyancy, *Mon. Wea. Rev.*, **110**, 504–520.